

PFC/JA-96-40

## Formation and Evolution of Internal Transport Barriers in Alcator C-Mod

D.T. Garnier, E.S. Marmor, C.L. Fiore, J.A. Goetz,  
S.N. Golovato,<sup>1</sup> M.J. Greenwald, A.E. Hubbard, J.H. Irby,  
P.J. O'Shea, J.J. Ramos, J.E. Rice, J.M. Schachter, P.C. Stek,  
Y. Takase, R.L. Watterson,<sup>2</sup> S.M. Wolfe, A. Martynov<sup>3</sup>

October 1996

<sup>1</sup>presently at Tokyo Electron America, Beverly, MA, USA.

<sup>2</sup>presently at CP Clare Corporation, Lexington, MA, USA.

<sup>3</sup>Keldysh Institute of Applied Mathematics, Moscow, Russia.

To be published in the Proceedings of the 16<sup>th</sup> IAEA Fusion Energy Conference.

This work was supported by the U. S. Department of Energy Contract No. DE-AC02-78ET51013. Reproduction, translation, publication, use and disposal, in whole or in part by or for the United States government is permitted.

## Formation and Evolution of Internal Transport Barriers in Alcator C-Mod \*

### Abstract

Central fueling of Alcator C-Mod plasmas with lithium and deuterium pellets often leads to a strong reduction of core energy and particle transport. These transient modes, which typically persist for a few energy confinement times, are characterized by the development, during the post-pellet reheat, of a very steep pressure gradient (scale length  $l_p \leq a/5$ ) in the inner third of the plasma. Inside of the transport barrier, the ion thermal diffusivity drops to values close to those predicted from neoclassical theory. The global energy confinement time shows an increase of about 30% relative to L-mode scaling. Sawtooth suppression is typical, but not observed in all cases. The addition of up to 3 MW of ICRF auxiliary heating, shortly after the pellet injection, leads to high fusion reactivity, with D-D neutron rates enhanced by a factor of about 10 over L-mode discharges with similar input powers. The measured current density profile shows that a region of reversed magnetic shear exists at the plasma core. The change in current profile is consistent with the calculated bootstrap current created by the pressure gradient. MHD stability analysis indicates that these plasmas are near both the  $n = \infty$  and the  $n = 1$  marginal stability limits.

### 1. INTRODUCTION

Pellet-fueling induced confinement enhancement was first seen in ohmic discharges on Alcator C [1] and was subsequently observed on other experiments. More recently, on JET, shear reversal in ICRF heated, pellet fueled, current-ramped discharges was reported [2,3], and the acronym, PEP, for Pellet Enhanced Performance, was coined to describe them. With 80 MHz fixed-frequency sources, ICRF heated PEP modes have been obtained, without current ramping, in two regimes on Alcator C-Mod: at 5.3 tesla, hydrogen minority deuterium majority heating has been used, while at 7.9 tesla, heating with  $^3\text{He}$  minority in deuterium majority plasmas was used.

### 2. EXPERIMENTAL OBSERVATIONS

Typical plasma parameters for a 7.9 tesla case are illustrated in figure 1. Time histories of the key core parameters for this  $I_p = 1$  MA case clearly show the peaking of density profile following the injection of a lithium pellet at 0.76 seconds.

Figure 2 compares the total plasma pressure profiles at 3 times in a discharge: during the pre-pellet ohmic phase; near the peak of the PEP mode phase; and following the collapse of the core and return to L-mode. It is apparent that the transport improvement is restricted to the inner half of the profile. With the measured temperature and density profile time histories, along with calculated ICRF power deposition and measured bolometric radiation profiles

---

\* Work supported by the U.S. Department of Energy, Contract No. DE-AC02-78ET51013.

as inputs, the TRANSP [4] code is used to calculate the evolution of transport coefficients as well as current density profiles. According to these calculations approximately 30% of the current density at  $\rho = 0.2$  is due to the pressure gradient driven bootstrap current, whose time history is shown in the second last panel of figure 1. The final panel of this same figure illustrates the time histories of  $q_0$  and  $q_{min}$ , consistent with the notion that the observed region of reversed shear is due to the increased bootstrap fraction.

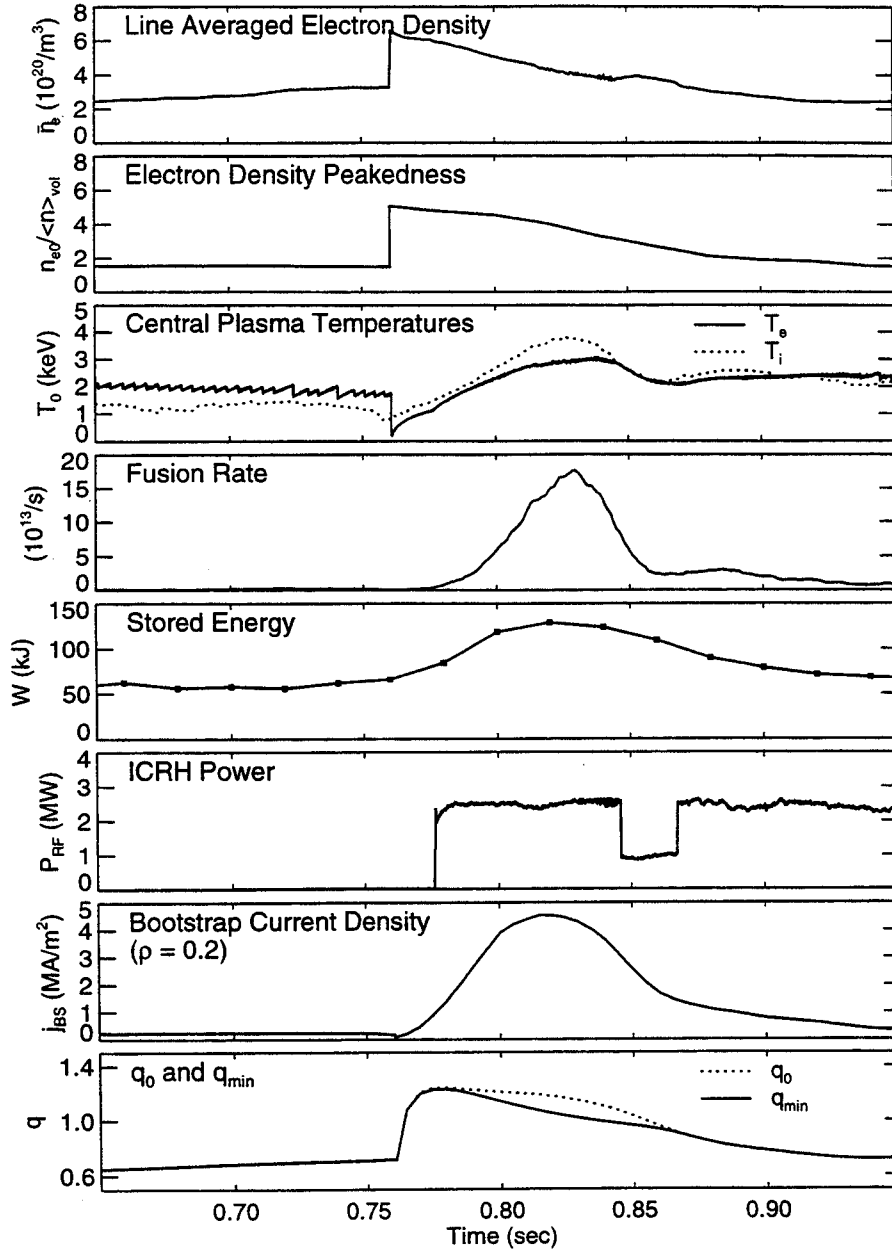


Figure 1. Time histories of plasma parameters for an 8 tesla, 1 MA PEP-mode shot. The lithium pellet was injected at 0.76 seconds. The time histories of bootstrap current density and  $q$  are calculated with TRANSP.

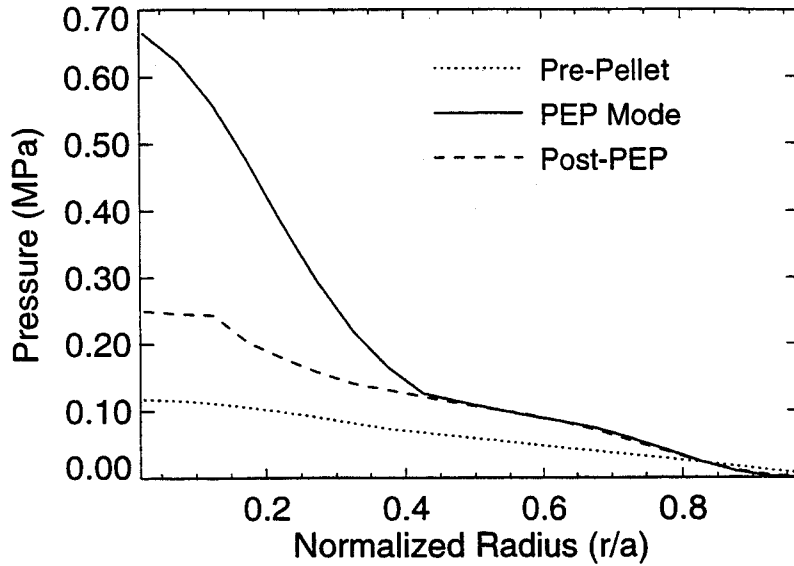


Figure 2. Pressure profiles at 3 times: pre-pellet; shortly after the peak in the neutron rate; and after the collapse to L-mode.

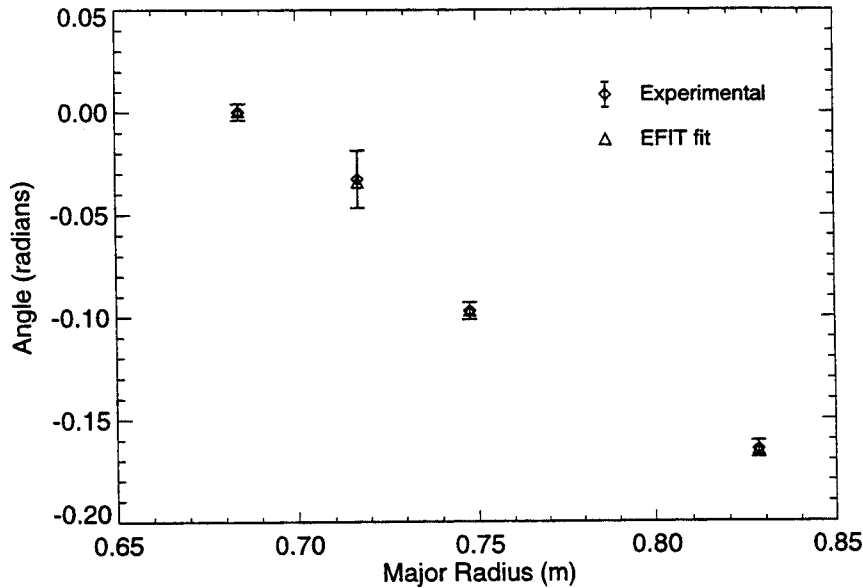


Figure 3. Comparison of measured magnetic field angle midplane profile with the fitted profile from the EFIT equilibrium reconstruction. The measurements are taken from a series of similar 5 tesla, 0.8 MA discharges, into which 2 lithium pellets were injected: the first to induce PEP-mode; the second to make the internal field measurements.

Internal poloidal magnetic field profiles are measured in Alcator C-Mod, at a single time point in a discharge, using a lithium pellet ablation trail imaging technique [5]. Figure 3 compares the measured total magnetic field angle,

obtained in this fashion on a sequence of 4 similar discharges, to the resulting EFIT [6] derived angles; the measured internal angles have been added as constraints for the EFIT reconstruction of the equilibrium. Figure 4 illustrates the corresponding current density and  $q$  profiles. The measurements were taken 75 ms after the injection of the pellet which induced the PEP transition, 10 ms after the peak in the fusion neutron rate. The hollow  $q$  profile is apparent, with  $q_0 = 2$  and  $q_{min}$  just larger than 1. This was a 5.3 tesla, 0.8 MA case. TRANSP calculations indicate that the current density profile is roughly consistent with that expected when bootstrap effects are included, with 1/4 of the current density at  $\rho = .3$  driven by the bootstrap current.

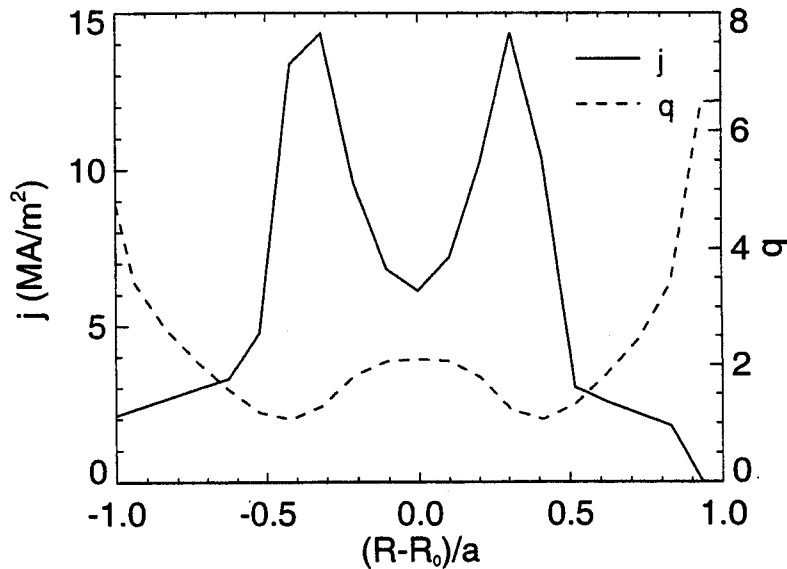


Figure 4. Current density and  $q$  profiles inferred from the midplane poloidal field profile measurements shown in figure 3. The measurements are made 10 ms after the peak neutron rate is reached.

All PEP modes are observed to be transient. On C-Mod, they typically last from 50 to 100 ms. This is comparable to the resistive time scale for the current profile to relax from reverse to normal shear, but cause and effect cannot be established without measurements of the current profile time evolution. Several phenomena can apparently be ruled out as the cause of the transition out of PEP mode. As seen on ECE and soft x-ray tomography diagnostics, there is often low  $m/n$  coherent MHD activity observed near the time of the transition back to L-mode; however, in many cases this activity appears to saturate long before the collapse, and in some cases it is absent. The resumption of sawtoothing does not always correlate with the end of the PEP phase; often, the pressure profile has relaxed back to those typical of L-mode, as much as 100 ms before sawtoothing resumes.

### 3. MHD STABILITY

To explore the ideal stability of C-Mod PEP mode discharges, the 7.9 tesla shot already described was analyzed using the CAXE and KINX [7] set of

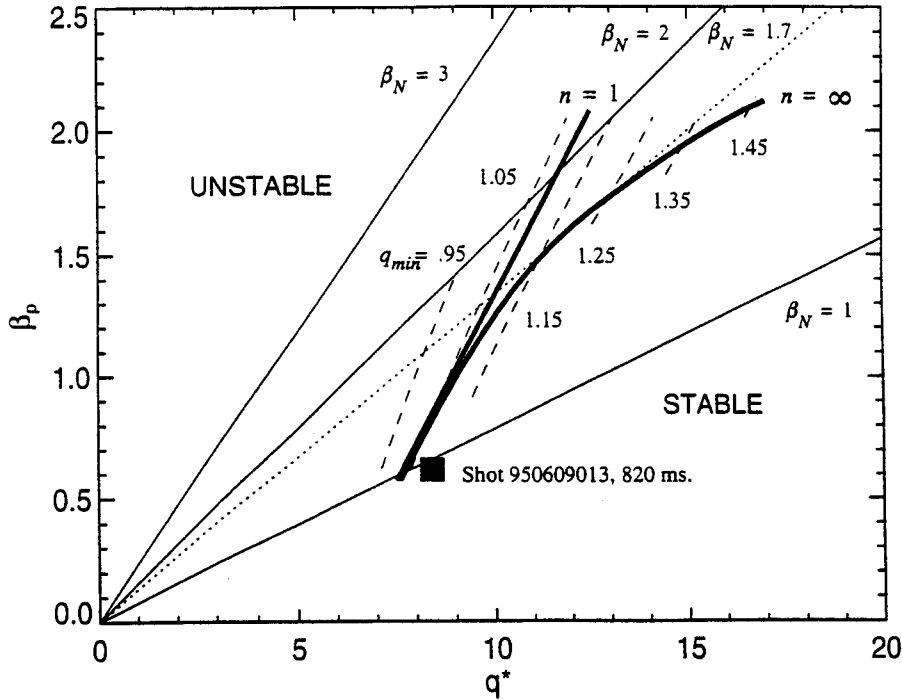


Figure 5. Ideal stability of an 8 tesla, 1 MA PEP-mode discharge (at 830 ms), and discharges with similar equilibria. Those equilibria falling to the left or above the heavy lines are unstable to ideal modes.

codes for equilibrium reconstruction and ideal MHD stability. Using  $q^*$  and  $\beta_p$  scalings, the stability of discharges over a range of these parameters, but with similar pressure and current density profiles, can be examined. Figure 5 shows the results of such an investigation, which indicate that the basis equilibrium is stable, but is very close to the marginal stability limits both for the  $n = 1$  kink and  $n = \infty$  ideal ballooning modes, as shown by the heavy lines. In all cases it is assumed that there is no conducting wall present. Thus a modest increase in the plasma  $\beta$ , or a slight drop in  $q_{min}$  could be expected to drive the discharge unstable. These results further indicate that, for this current density profile, a  $\beta$  limit exists for the  $n = \infty$  modes for  $\beta_N \gtrsim 1.7$ ; discharges with higher normalized  $\beta$  should be unstable to the high- $n$  ballooning modes for values of  $q_{min}$  up to 1.5. Discharges with  $q_{min} > 2$  and small or negative central shear enter the region of “second stability” and are stable to high- $n$  ballooning modes even with large values of  $\beta$ .

#### 4. DISCUSSION

There has recently been much attention focussed on reverse shear configurations and resultant improvements in confinement [8,9]. Typically, these NCS/ERS discharges have many, if not all, of the macroscopic characteristics of PEP mode discharges; NCS/ERS is accessed by tailoring the initial growth of the plasma to freeze in a hollow current profile, followed by strong neutral beam heating. The relative importance of the central fueling from the beams in ac-

cessing NCS/ERS is not known; however, this fueling cannot be separated from the central heating when NBI is the main auxiliary heating source. It is well established that reverse shear alone is not sufficient to achieve the transition. Other modes of enhanced core confinement have also been identified, including the high  $\beta_p$  modes on JT-60U [10] and JET [11], and the CH-Mode on PBX-M [12]. In all of these cases, areas of commonality include enhanced particle and energy confinement, with highly peaked core pressure profiles. In most, if not all cases, core fueling appears to play an important role, either through pellet or beam particle deposition. If it turns out that central particle fueling is one of the necessary conditions to access these enhanced core confinement modes, then extrapolation to future devices, such as ITER, may be very difficult.

- [1] M. Greenwald, et al., Phys. Rev. Lett. **53**(1984)352.
- [2] M. Hugon, et al., Nuclear Fusion **32**(1992)33.
- [3] P. Smeulders, et al., Nuclear Fusion **35**(1995)225.
- [4] R. Hawryluk, Physics of Plasmas Close to Thermonuclear Conditions, Proceedings of the Course held in Varenna, Italy 1979, edited by B. Coppi, (Commission of the European Communities, Brussels, 1980) Vol. 1 , p.19
- [5] J.L. Terry, et al., Rev. Sci. Instrum. **63**(1992)5191.
- [6] L.L. Lao, et al., Nuclear Fusion **30**(1990)1035.
- [7] S. Medvedev, et al., in Proc. 20th EPS Conf. on Controlled Fusion and Plasma Phys., Lisbon, (1993)1279.
- [8] E.J. Strait, et al., Phys. Rev. Lett. **75**(1995)4421.
- [9] F.M. Levinton, et al., Phys. Rev. Lett. **75**(1995)4417.
- [10] T. Nishitani, et al., Nuclear Fusion **34**(1994)1069.
- [11] B.W. Stallard, et al., Bull. Am. Phys. Soc. **40**(1994).
- [12] PBX-M Group, Fusion Engineering Design **26**(1995)83.